Out of phase multiaxial fatigue strength of cast iron

M.E. Cristea[1], S. Foletti[2], C. Cagdas[2]

[1]TENARIS Dalmine, R&D, Piazza Caduti 6 Luglio 1944, I-24044 Dalmine, Italy, mcristea@tenaris.com, Tel: +39 (035) 560 2656, Fax: +39 (035) 560 2845
[2]Politecnico di Milano, Department of Mechanical Engineering, Via La Masa 1, I-20156 Milano, Italy, stefano.foletti@polimi.it, Tel: +39 (022) 399 8629

ABSTRACT. *High-cycle fatigue behaviour of a ductile cast iron has been investigated under multiaxial out-of-phase loading. An experimental plan aimed to study the effect of both complex loadings and presence of imperfections in the materials was carried out. It has been found that the compressive stress decreases the shear stress amplitude limit. Microshrinkages formed in the casting process have also a detrimental effect on fatigue behaviour. Moreover, a hybrid approach which links together the influence of shrinkage porosity size on fatigue limit and multiaxial fatigue strength has been applied. The selected integral approach showed a good agreement with the experimental data for different loading conditions.*

INTRODUCTION

Many mechanical components are produced by casting, a process widely used in the automotive and railway industries [1], as well as in tooling manufactures such as rolling rolls and rolling bearings. Rolling contact fatigue (RCF) is traditionally a very critical load condition for as cast components, which always contain microshrinkage porosities exposed to the out-of-phase stresses occurring below the surface of contacting bodies. Therefore, fatigue assessment becomes a complex issue to be treated considering the interaction between the different involved variables [2].
The purpose of this work is to understand the behaviour of a ductile cast iron for rolling rolls under RCF condition. An experimental plan based on pure axial and torsional cyclic loads, as well as multiaxial loadings, simulating conditions of sub-surface RCF, with axial force always in compression and shifted on 90° relatively to the torsional cycle, has been carried out. In all the specimens, taken from industrial castings, shrinkage porosities with irregular shapes and a broad size range have been observed. An effort has been devoted to estimate the characteristic size through the "statistic of extremes".
An integrated approach is proposed to predict the fatigue strength under out of phase multiaxial loading for as-cast materials. This methodology is based on the application of a multiaxial fatigue criterion used in conjunction with the Murakami's concept [3] in order to take into account the variation of the fatigue limits with porosity dimension.

EXPERIMENTAL

Material

The material investigated is a commercial ductile cast iron with a pearlite matrix and uniform distributed spheroidal graphite nodules, identified as SF. Its chemical composition and mechanical properties match those of an ISO Standard 1083:2004 class of 700-2 cast iron [4].

Fatigue tests

Pure tension–compression and alternating torsion, as well as multiaxial tests, were conducted in load control mode on small round specimens with different diameters of the gauge section, namely 7 mm for tension-compression axial tests and 16 mm for torsional and multiaxial ones. For torsional and multiaxial tests a servohydraulic biaxial test system Walter + Bai LFV250–T2200, with axial loads up to 250 kN and torques up to 2200 Nm with ±50° torsional angle was used. The pure axial tests were performed by a Rumul machine with maximum load up to ± 50 kN.

In the biaxial fatigue tests, the aforementioned specimens were subjected to alternating torsion and pulsating compression applied with a 90° phase shift. The stresses can be written as:

$$\begin{aligned} \sigma &= \sigma_m + \sigma_a \cos \omega t \\ \tau &= \tau_a \sin \omega t \end{aligned} \tag{1}$$

where $\sigma_m = -\sigma_a$ is the mean stress, σ_a is the axial stress amplitude, and τ_a is the shear stress amplitude.

The stress–time histories of Eq. 1 are graphically reported in Figure 1 in terms of force and torque path.

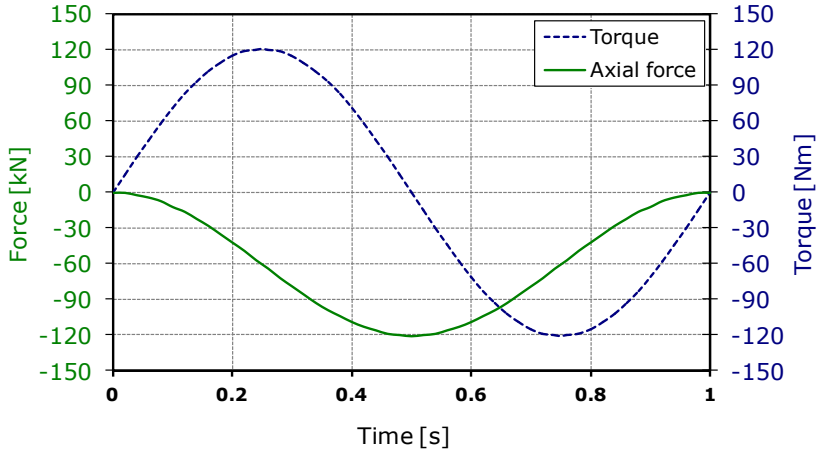

Figure 1. Typical stress–time history corresponding to the alternating torsion and pulsating compression applied to the specimens.

RESULTS

Fatigue limits

The results of pure axial and torsional fatigue limits are reported in Table 1 denoted as σ_w and τ_w respectively. These fatigue limits were evaluated by adopting the staircase method, a number of 10 specimens being used for each limit. The run-out condition has been assumed when the specimen survived more than 10^7 cycles.

Table 1. Amplitude fatigue limits under pure loads

$R=\frac{\sigma_{min}}{\sigma_{max}};\frac{\tau_{min}}{\tau_{max}}$	Axial fatigue limit σ_w (MPa)	Torsional fatigue limit τ_w (MPa)	τ_w/σ_w
-1;-1	197	178	0.9

For the multiaxial tests, the stress path conditions have been chosen in order to replay the critical state of the component during real service. These tests produced in the specimens a non-proportional stress state of only two of the six stress tensor components that are present under rolling contacts: the alternating shear stress and pulsating compressive stresses (Figure 1).

Two levels of the ratio R, between minimum axial stress (σ_{min}) and amplitude of shear stress (τ_a) were chosen, similar with that observed during the stress state analysis of the component. In particular, fatigue limit for R = -3 and R = -4 has been experimentally determined by stair case method, the limit conditions for shear stress denoted as τ_{wm} are reported in Table 2. As expected, the allowable shear stress amplitude decreases with increasing out-of-phase compressive loads.

Table 2. Shear stress amplitude at fatigue limits under multiaxial loads

$R=\frac{\sigma_{min}}{\tau_{amp}}$	Minimum axial stress, σ_{min} (MPa)	Torsional fatigue limit τ_{wm} (MPa)
-3	-402	134
-4	-430	108

Shrinkage porosities on fracture surfaces

After fatigue testing, all surfaces of broken specimens have been examined by means of Scanning Electron Microscope (SEM). It has been observed that in all cases the fatigue cracks initiated from the largest microshrinkages, which after growth, lead to the failure of the specimens. The location (at the specimen surface or within the bulk) and the size of each initiation site were observed and measured. In Figure 2, examples of the manufacturing imperfections are reported for both axial specimens and multiaxial ones. Difficulties to found the evidence of the shrinkages has been encountered for torsional limit specimens due to the fracture surface plan at 45°.

In order to identify the typical maximum porosity size present in the specimens, the microshrinkages have been measured in terms of square root of area (√area) by means of a commercial software, after manual drawing of the shrinkage porosity edges on the SEM images, as shown in Figure 2b.
The measurements have been analysed by the use of "statistics of extremes" which is based on recording only the maximum defect size in a given control area (e.g. the specimens fracture surface). The data so-obtained are then analysed with the Largest Extreme Value Distribution ("LEVD") in order to estimate the characteristic dimension of the maximum porosity occurring in a large volume.
Figure 3 reports the measured data plotted as √area size in the Gumbel probability plot.
It can be noted a good repeatability of the measurements between multiaxial and axial failed specimens, the mean values being nearly the same: √area=1100 μm.

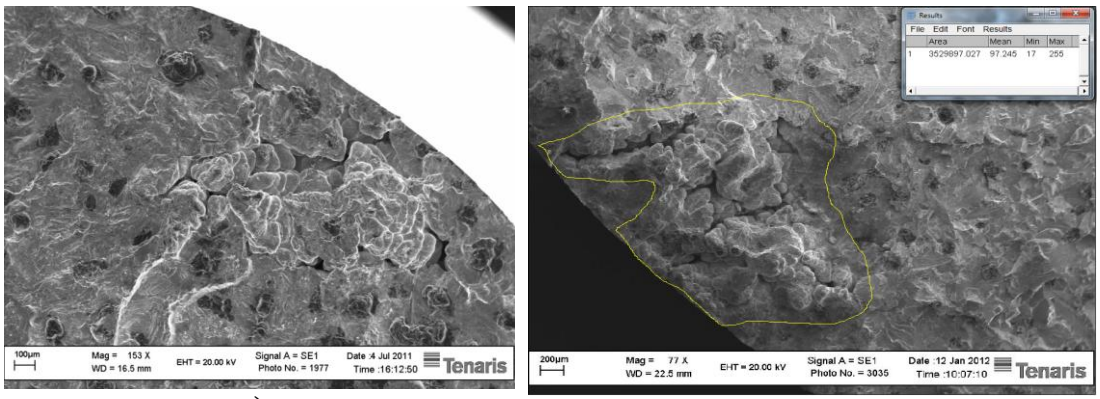

a) b)

Figure 2. Typical fracture surfaces on specimens containing microshrinkages porosities: a) specimen under pure axial load; b) specimen under multiaxial loads.

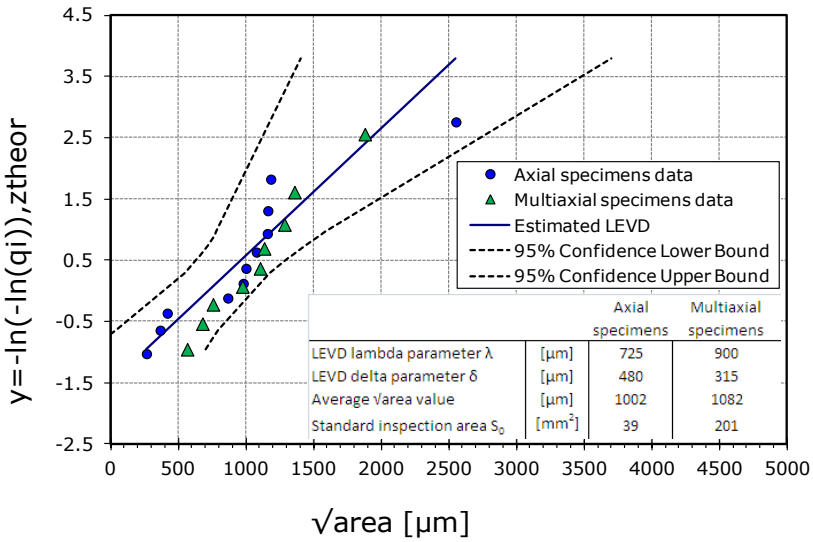

Figure 3. LEVD analysis of shrinkage porosity data measurements.

As already mentioned before, taking into account that all specimens failed due to the fatigue growth of a crack initiated at a pre-existent casting porosity, it is evident that the fatigue limits for both pure loading conditions and multiaxial stress state (reported in Table 1 and Table 2, respectively) are strongly dependent of the porosity size.

FATIGUE LIMIT PREDICTION

Axial and torsional loadings

Under pure loadings, the well known and widely used Murakami and Takahashi model [3] can be used by means of empirical equation based on √area parameter (the square root of the surface of the defect in the plane perpendicular to the maximum principal stress direction) to predict the fatigue limit of material containing defects. This model takes into account the effect of mean stress.

The fatigue limits for tension (σ_w) and torsion (τ_w) are given by Eq. 2:

$$\sigma_w = \frac{1.43\left(H_V + 120\right)}{\left(\sqrt{area}\right)^{1/6}}\left[\frac{1-R}{2}\right]^n ; \tau_w = \frac{1.22\left(H_V + 120\right)}{\left(\sqrt{area}\right)^{1/6}}\left[\frac{1-R}{2}\right]^n \quad (2)$$

with $n = 0.226 + H_V 10^{-4}$, H_v = 298 Vickers hardness for the investigated cast iron [5].

Considering a mean value of the √area=1100 mm (see Figure 3) it can be observed that the model predicts quite well the fatigue limit for the axial load but calculation is less good for the torsional one (Figure 4). This occurs because under torsional loads the tortuous nature of the fracture surface does not allow an accurate defect size measurement as well as defect site identification.

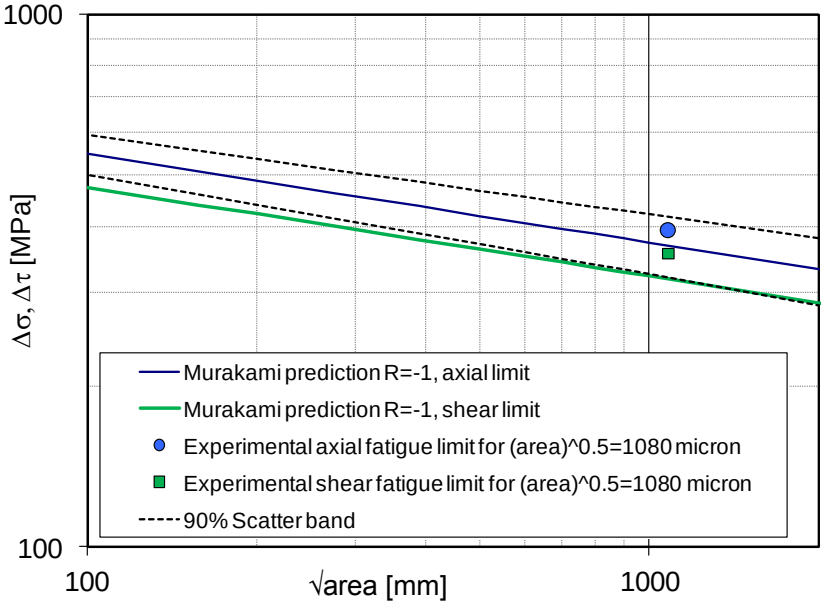

Figure 4. Murakami's model prediction compared to experimental data for pure axial and torsional loads: fatigue limit vs porosity size.

Multiaxial fatigue criterion

An integral approach method has been applied for multiaxial loadings conditions, where the equivalent stress acting on a plane is calculated within a specified volume and integrated over all possible planes. The integral approach was selected because the use of a critical plane approach becomes difficult for materials containing defects as the applied stresses give rise to a stress gradient on the material.

Following this approach, among all different methods available in the literature [2,6,7], Papadopoulos criterion was selected due to its high applicability to non proportional multiaxial loading conditions. According to Papadopoulos [8] the accumulated plastic strain is proportional to the shear stress amplitude, τ_a, and independent from the mean shear stress τ_m. The general formulation of the criterion for avoiding a fatigue failure is:

$$\sqrt{\langle T_n^2 \rangle} + \alpha \sigma_{H,\max} \leq \beta \tag{3}$$

where: $\sqrt{\langle T_n^2 \rangle}$ is the average value of the resolved shear stress amplitudes T_n^2 acting over all the possible glide systems of an elementary volume V; α and β are material constants determined through experimental fatigue tests, β is the torsional fatigue limit at R=-1 and α is a function of both axial and torsional fatigue limits at R=-1.

$$\alpha = \frac{3\tau_w}{\sigma_w} - \sqrt{3}; \beta = \tau_w \tag{4}$$

Under out-of-phase condition for axial and torsional loading, as reported in [8], $\sqrt{\langle T_n^2 \rangle}$ becomes:

$$\sqrt{\langle T_n^2 \rangle} = \sqrt{\frac{\sigma_a^2}{3} + \tau_a^2} \tag{5}$$

and the maximum hydrostatic stress equal to:

$$\sigma_{H,\max} = \frac{\sigma_a + \sigma_m}{3} \tag{6}$$

Therefore, substituting Eq. 5 and Eq. 6 in Eq. 3, the formula becomes:

$$\sqrt{\frac{\sigma_a^2}{3} + \tau_a^2} + \alpha \frac{\sigma_a + \sigma_m}{3} \leq \beta \tag{7}$$

Multiaxial fatigue criterion for materials containing defects

After determining the typical defect size found in the material as reported in the previous section, a hybrid approach based on determining the influence of defect presence on multiaxial fatigue limit has been adopted. This concept, already used by Nadot et al. [2], is aimed to link an empirical relation characterising the influence of defect size on fatigue limit, through Murakami's approach and a multiaxial endurance criterion through Papadopoulos integral approach used in the present study.

The connection between the two approaches can be made in two ways:

- Directly, considering the fatigue limit values σ_w and τ_w to be used in Eq. 8 as a function of defect size;

- Indirectly, correlating σ_w and τ_w to material parameters D and G, describing the influence of the defect √area on the fatigue limit as follows:

$$\sigma_D = \frac{D}{\left(\sqrt{area}\right)^{1/n}}, \tau_D = \frac{G}{\left(\sqrt{area}\right)^{1/n}} \quad (8)$$

The combination of Murakami's empirical relation and Papadopoulos's model leads to identifying the material parameters α and β using the experimental results from Eq. 8. Through this approach each single fatigue path shown in Figure 5 can be related with defect size and the following parameters can be determined:

- the allowable maximum defect size, given as input the loading conditions;
- the critical loading condition, given as input the defect size.

Increasing the defect size, a reduced safe region is observed. In Figure 6, the experimental results (from Table 2) are compared with the model predictions. For R=-4 a difference between calculated and experimental defect size of 18% has been found (Figure 6a), whereas for R=-3 a very good agreement with the prediction can be noted (Figure 6b).

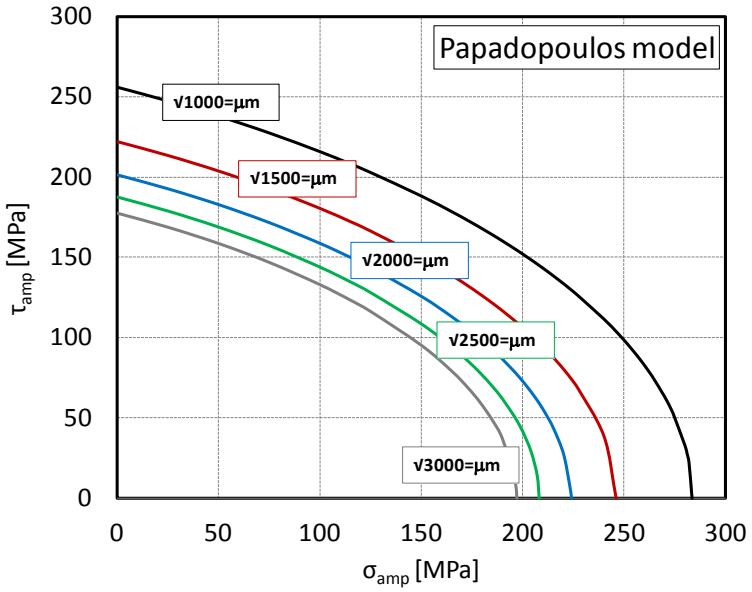

Figure 5. Papadopoulos model predictions as a function of defect size.

CONCLUSIONS

High cycles fatigue tests have been carried out on ductile cast iron under both pure tensile and torsional stresses and multiaxial out-of-phase loadings. Furthermore, a predictive model able to integrate complex loading on a material containing defects has been applied. It has been found that:

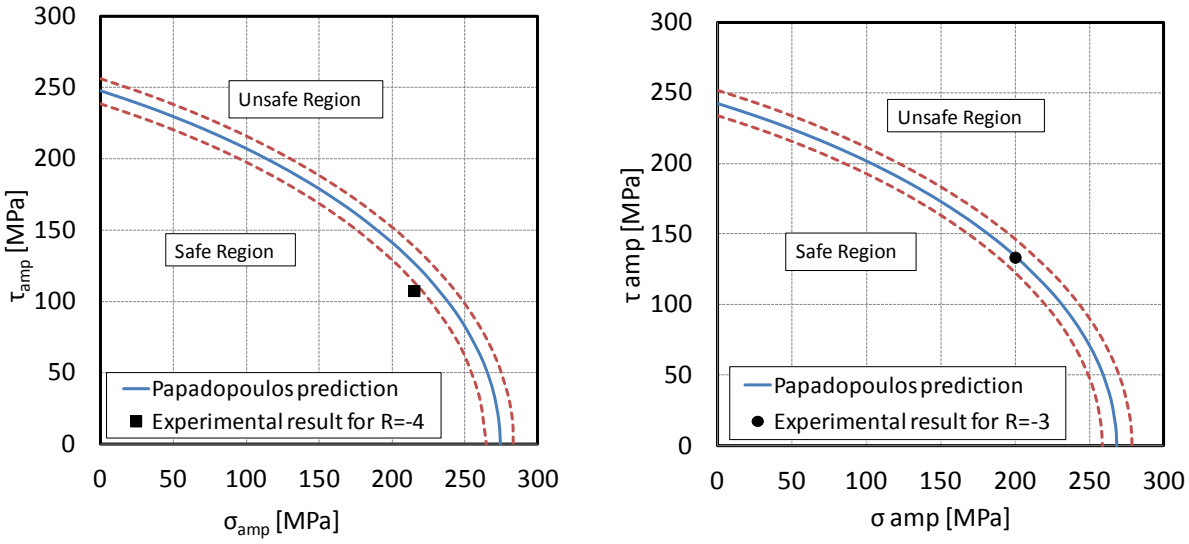

Figure 6. Experimental results vs. prediction model: a) R=-4; b) R=-3.

- the presence of microshrinkages is origin of fatigue initiation and growth which leads to specimens failure;
- a statistical analysis based on fracture surface examination for maximum defect measurement showed a typical average defect size of 1100 μm (√area);
- good agreement between experimental pure loading fatigue limits and Murakami's prediction model has been found;
- Papadopoulos integral approach combined with the Murakami's model leads to a predictive hybrid model for multiaxial loading in presence of defects. Also in this case, a good agreement with the experimental multiaxial fatigue limits for two different loading conditions has been found;
- under multiaxial loadings, the compressive stress on the shear stress amplitude showed a detrimental effect on fatigue limit results.

REFERENCES

1. Bernasconi, A., Filippini, M., Foletti, S., Vaudo, D. (2006) *Int J Fatigue* **28**, 663–672.
2. Nadot, Y., Denier, V. (2004) *Eng Fail Anal* **11**, 485–499.
3. Murakami, Y. (2002) *Metal fatigue: effect of small defects and non metallic inclusions*, Elsevier editor.
4. Davis, J. R. (1996) *ASM Specialty Handbook: Cast Irons*, ASM International.
5. Beretta, S. (2003) *Fatigue Fract Eng Mater Struct* **26**, 551-559.
6. Nadot, Y., Mendez, J., Ranganathan N. (2004) *Int J Fatigue* **26**, 311–319.
7. Bernasconi, A., Foletti, S., Papadopoulos, I.V. (2008) *Int J Fatigue* **30**, 1430–1440.
8. Papadopoulos, I.V. (1994) *Int J Fatigue*, **16**, 337-384.